THREE-DIMENSIONAL TURBULENT STRUCTURES OF DIFFERENT SCALES

Akira Rinoshika*, Yu Zhou**

*Department of Mechanical Systems Engineering, Yamagata University, Yamagata, Japan
**Department of Mechanical Engineering, The Hong Kong Polytechnic University, Hong Kong

<u>Summary</u> An orthogonal vector wavelet multi-resolution technique has been developed and applied to decomposing the measured velocity data of a three-dimensional turbulent near-wake into a number of wavelet components based on their central frequencies or scales. The spanwise vorticity contours of the wavelet component at f_0 (the vortex shedding frequency) display a secondary spanwise structure near the saddle point, whose vorticity is opposite-signed to that of the Karman vortices. The wavelet components of f_0 or $2f_0$ make a predominant contribution to the Reynolds normal stresses and account for most of the shear stress. On the other hand, the relatively small-scale turbulent structures contribute most to vorticity variance.

INTRODUCTION

The turbulent near-wake of a circular cylinder is characterised by a high degree of organisation, thus being attractive for studying turbulent structures in terms of their organised aspects and clarifying their role in the transport process. In this flow, turbulent structures consist of a wide range of scales, including large-scale spanwise structures and relatively small-scale structures such as the secondary vortices, Kelvin-Helmholtz vortices and longitudinal rib-like structures. Previous studies [1], [2] of the organised motion mostly focused on large-scale structures; investigations of other scales have been relatively scarce since it is difficult to extract the structures of these scales using conventional vortex-detection techniques. The purpose of the present work aims to develop an orthogonal vector wavelet multi-resolution technique for decomposing the turbulent structures of different scales and provides both quantitative and qualitative information on the structures of individual scales. The turbulent structures of various scales are examined in detail, including their instantaneous streamline patterns and vortcity contours, and contributions to Reynolds stresses and root mean square (rms) vorticity from each scale.

ORTHOGONAL VECTOR WAVELET MULTI-RESOLUTION TECHNIQUE

For any one-dimensional vector data \vec{v} , the vector discrete wavelet transform, $\vec{S} = W\vec{v}$, is first carried out. Here S and W are called discrete wavelet coefficient matrix and the analysing wavelet matrix of \vec{v} . W is orthogonal and satisfies $W^TW = I$, where I is a unit matrix, usually constructed based on a cascade algorithm of an orthogonal wavelet basis function. In the present study, the Daubechies wavelet basis with an order of 20 is used. Then the inverse vector discrete wavelet transform is applied to the wavelet coefficient of each wavelet level and the wavelet components of

wavelet components at different wavelet level or central frequencies, i.e., $\vec{v} = \sum_{i=1}^{N} \vec{v}_i$, where the vector wavelet

vector data are constructed. Therefore, a non-linear vector data can be convert to an infinite summation of vector

components are normal to each other, given by $\overrightarrow{v_i} = W^T \overrightarrow{S_i}$. The first term $\overrightarrow{v_1}$ and the last $\overrightarrow{v_N}$ represent the wavelet components at level 1 (the lowest frequency) and level N (the highest frequency), respectively. Evidently, the sum of all wavelet level or frequency components is a reconstruction of the original vector data.

EXPERIMENTAL CONDITIONS

A circular cylinder (d = 12.5 mm) was used to generate a turbulent wake. Measurements were conducted at x/d = 20 (x is the streamwise distance downstream of the cylinder) and a constant free stream velocity ($U_{\infty} = 6.7$ m/s). The corresponding Reynolds number Re ($\equiv U_{\infty}d/v$) was 5600. The Kolmogorove length scale at this x/d was estimated to be about 0.16 mm. Two orthogonal arrays, each of eight X-wires, were used. Eight X-wires were aligned in the (x, y)-plane, i.e. the plane of mean shear, and eight in the (x, x)-plane, which is parallel to both the cylinder axis and the streamwise direction. The sixteen X-wires allow velocity fluctuations x and y in the (x, y)-plane and y and y in the (x, y)-plane to be obtained simultaneously. The sampling frequency was 3.5 kHz.

INSTANTANEOUS TURBULENT STRUCTURES OF VARIOUS SCALES

The dominant frequency f_0 of large-scale structures (i.e. Kàrmàn vortices) is selected as the 'fundamental central frequency' for the wavelet multi-resolution analysis, and the central frequencies of wavelet components are given by f_0 , $2f_0$, $4f_0$ and $8f_0$. This range of frequencies is of major concern in the present investigation. In order to better 'visualise data', sectional streamlines [3] were constructed for velocity of each scale as well as for measured velocities. The streamlines are viewed in a reference frame translating at the convection velocity of the large-scale structures, which is $U_c = 0.87U_{\infty}$. Vorticity was approximated based on instantaneous wavelet components of velocity using the central difference approximation [1]. Figures 1 and 2 show instantaneous streamlines and corresponding normalised vorticity contours of different scales in the (x, y)- and (x, z)-plane, calculated from the wavelet components of velocity at the central frequencies of f_0 and f_0 , respectively. The solid and broken lines in the vorticity contours represent positive and negative levels, respectively. Structures at f_0 represent the large-scale organised motion and appear better organised and exhibit a much stronger periodicity. The foci and saddle points are marked by f_0 and f_0 , respectively. A number of more

observations can be made from Fig.1. Firstly, the focus in general coincides with the local peak of $(\omega_z)_{f_0}d/U_\infty$ (negative), while the saddle point occurs at the minimum of $(\omega_z)_{f_0}d/U_\infty$. Secondly, the saddle point is mostly associated with the up-down concentrations of positive vorticity, e.g. at $tU_c/d \approx -8$, -4, 0.8 and 5.2 in Fig.1 (c). The positive vorticity concentration below the saddle point is apparently part of positive-sign vortices, which occur below the centreline. On the other hand, the vorticity concentration above the saddle point probably results from interactions between two consecutive spanwise structures of negative sign; its positive sign is further consistent with the fact that the vorticity strength of a spanwise vortex is higher than that of the neighbouring downstream one because of a fast decay in the vortex strength as x/d increases. This secondary structure of positive vorticity (or negative-sign vorticity if below the centreline) has not been observed from previous conditional method [1], [2].

As the central frequency increases to $2f_0$ (Fig.2), the vorticity strength in both planes almost doubles that at the central frequency of f_0 , though this strength in the (x, z)-plane is still significantly weaker than in the (x, y)-plane, the maximum contour level of $(\omega_y)_{2f_0} d/U_\infty$ being 0.7, significantly smaller than that (1.2) of $(\omega_z)_{2f_0} d/U_\infty$. The difference

reflects the fact that the structures in the (x, y)-plane are connected to primary or secondary spanwise structures, while those in the (x, z)-plane result from the three dimensionality of primary spanwise structures and rib structures. Furthermore, the vorticity concentrations of opposite sign tend to occur alternately in the longitudinal direction, irrespective of the (x, y)- or (x, z)-plane. The alternate occurrence of opposite-sign vorticity concentrations, mostly associated with the saddle points, is also observed in the spanwise direction. The spanwise spacing between these concentrations is in the order of 1d. The observation is again linked to the behaviour of the rib structures.

The contributions to the Reynolds stresses from the wavelet components are also quantified. The wavelet components of f_0 and $2f_0$ contribute most to the Reynolds normal stresses, accounting for about 45% of u^2 and 80% of v^2 , respectively. The contribution from the wavelet component of $4f_0$ declines quite sharply, by up to 30% of v^2 , compared with that of f_0 or $2f_0$, and further reduces for a higher central frequency. The Reynolds shear stress is largely attributed to the wavelet components of lower central frequencies. The components of f_0 and f_0 are responsible for almost 70% of f_0 , the latter two components contributing about 35% to f_0 .

As to the root mean square vorticity of each scale, the wavelet component of f_0 makes a small contribution to spanwise vorticity variance, accounting for about 10% of $\overline{\omega_z^2}$. The contribution climbs as the central frequency increases; the component of $8f_0$ contributes about 22% to $\overline{\omega_z^2}$, suggesting that vorticity tends to reside in the small-scale structures.

CONCLUSIONS

- (1) The spanwise vorticity contours at f_0 display a secondary spanwise structure above the saddle point, whose vorticity is opposite-signed to that of the spanwise structures. This structure is observed for the first time and probably results from the strong interactions between the consecutive spanwise structures of the same sign. Its occurrence and vorticity sign is consistent with the downstream decay in the vorticity strength of the spanwise structures.
- (2) The wavelet components of f_0 or $2f_0$ make a predominant contribution to the Reynolds stresses.
- (3) The relatively small-scale turbulent structures contribute most to vorticity variance.

References

- [1] Hussain A.K.M.F., Hayakawa M.: Education of large-scale organized structures in a turbulent plane wake. J. Fluid Mech 180: 193-229, 1987.
- [2] Zhou Y., Antonia R.A.: A critical points in a turbulent near-wake. J. Fluid Mech 275: 59-81, 1994.
- [3] Perry, A. E., Chong, M. S.: A description of eddy motions and flow patterns using critical-point concepts. Ann. Rev. Fluid Mech 19: 125-155, 1987.

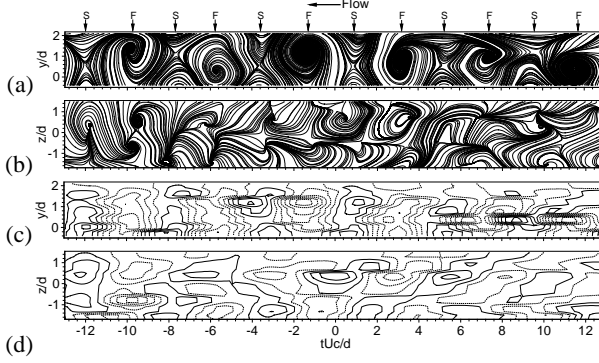


Fig.1 Instantaneous sectional streamlines of f_0 : (a) in the (x, y)-plane; (b) in the (x, z)-plane of y/d=0.2. Vorticity contours of f_0 : (c) $\left(\omega_z\right)_{f_0}d/U_\infty$ in the (x, y)-plane (Max: 0.45, Min: -

0.65, Increment: 0.1); (d) $(\omega_y)_{f_0} d/U_{\infty}$ in the (x, z)-plane of y/d=0.2 (Max: 0.35, Min: -0.35, Increment: 0.1)

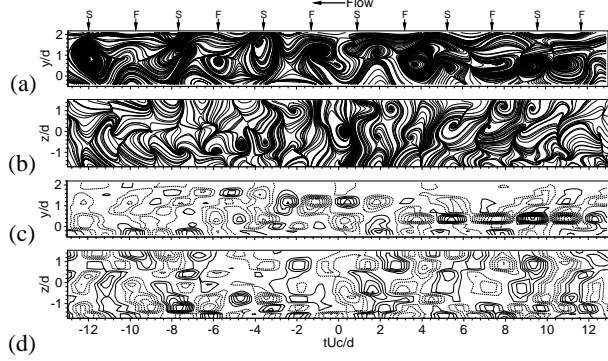


Fig.2 Instantaneous streamlines of $2f_0$: (a) in the (x, y)-plane; (b) in the (x, z)-plane of y/d=0.2. Vorticity contours of $2f_0$: (c) $(\omega_z)_{2f_0}d/U_{\infty}$ in the (x, y)-plane (Max: 1.0, Min: -1.2, Increment: 0.1); (d) $(\omega_y)_{2f_0}d/U_{\infty}$ in the (x, z)-plane of

y/d=0.2 (Max: 0.7, Min: -0.6, Increment: 0.1).